Interaction of Mutant Influenza Virus Hemagglutinin Fusion Peptides with Lipid Bilayers: Probing the Role of Hydrophobic Residue Size in the Central Region of the Fusion Peptide†

Xing Han,‡ David A. Steinhauer,§ Stephen A. Wharton,§ and Lukas K. Tamm*,‡

Department of Molecular Physiology and Biological Physics and Center for Structural Biology, University of Virginia Health Sciences Center, Box 10011, Charlottesville, Virginia 22906-0011, and Division of Virology, National Institute for Medical Research, The Ridgeway, Mill Hill, London NW7 1AA, United Kingdom

Received June 1, 1999; Revised Manuscript Received August 30, 1999

ABSTRACT: The amino-terminal region of the membrane-anchored subunit of influenza virus hemagglutinin, the fusion peptide, is crucial for membrane fusion of this virus. The peptide is extruded from the interior of the protein and inserted into the lipid bilayer of the target membrane upon induction of a conformational change in the protein by low pH. Although the effects of several mutations in this region on the fusion behavior and the biophysical properties of the corresponding peptides have been studied, the structural requirements for an active fusion peptide have still not been defined. To probe the sensitivity of the fusion peptide structure and function to small hydrophobic perturbations in the middle of the hydrophobic region, we have individually replaced the alanine residues in positions 5 and 7 with smaller (glycine) or bulkier (valine) hydrophobic residues and measured the extent of fusion mediated by these hemagglutinin constructs as well as some biophysical properties of the corresponding synthetic peptides in lipid bilayers. We find that position 5 tolerates a smaller and position 7 a larger hydrophobic side chain. All peptides contained segments of α-helical (33−45%) and β-strand (13−16%) conformation as determined by CD and ATR-FTIR spectroscopy. The order parameters of the peptide helices and the lipid hydrocarbon chains were determined from measurements of the dichroism of the respective infrared absorption bands. Order parameters in the range of 0.0−0.6 were found for the helices of these peptides, which indicate that these peptides are most likely aligned with their α-helices at oblique angles to the membrane normal. Some (mostly fusogenic) peptides induced significant increases of the order parameter of the lipid hydrocarbon chains, suggesting that the lipid bilayer becomes more ordered in the presence of these peptides, possibly as a result of dehydration at the membrane surface.

The highly conserved fusion peptide of influenza virus hemagglutinin (HA)[1] plays a crucial role in the mechanism of membrane fusion of this virus for gaining entry into infected host cells. This peptide comprises approximately 20 residues at the extreme N-terminus of the HA2 subunit of HA. The peptide interacts with the target membrane of host cells after a conformational change is induced in HA by low pH. To elucidate the structural basis of the fusogenicity of the influenza fusion peptide, the conformation and orientation of this peptide in lipid bilayers has been studied by many groups using CD, ATR-FTIR, and EPR spectroscopy (*1*−*9*). Even though there is general agreement that the HA fusion peptide adopts a predominantly α-helical conformation in lipid bilayers and orients obliquely to the membrane plane, the details of the structure of the fusion peptide and its interaction with lipid bilayers are less well understood. It has been proposed that the α-helical structure is required for fusogenic activity of the fusion peptide (*2*). More recently, we reported that the influenza virus fusion peptide also contains some β-structure, in addition to about 40−50% α-helical secondary structure (*8*).

One approach to further elucidating structure−function relationships of the fusion peptide in lipid bilayers is to study structural and other biophysical parameters of mutant fusion peptides with alterations of their sequence that abolish the fusion activity of the corresponding expressed hemagglutinins. The N-terminal glycine has great importance in determining the fusion activity of the HA. Only mutation to an alanine results in an HA with fusion activity; all other mutations greatly impair fusion (*10*−*12*). Probing the role of the glycine at the extreme N-terminus by this approach, we found that most mutations in this position increased the

† Supported by NIH Grant AI30557.

* To whom correspondence should be addressed. Telephone: (804) 982-3587. Fax: (804) 982-1616. E-mail: lkt2e@virginia.edu.

‡ University of Virginia Health Sciences Center.

§ National Institute for Medical Research.

[1] Abbreviations: ATR, attenuated total reflection; CD, circular dichroism; ELISA, enzyme-linked immunosorbent assay; EPR, electron paramagnetic resonance; FTIR, Fourier transform infrared; HA, hemagglutinin; DMEM, Dulbecco's Modified Eagle's Medium; DMPC, dimyristoylphosphatidylcholine; DMSO, dimethyl sulfoxide; HEPES, *N*-(2-hydroxyethyl)piperazine-*N*′-2-ethanesulfonic acid; MES, 2-(*N*-morpholino)ethanesulfonic acid; PBS, phosphate-buffered saline [10 mM sodium phosphate (pH 7.4), 0.137 M NaCl, and 2.7 mM KCl].

10.1021/bi991232h CCC: $18.00
Published on Web 10/23/1999

relative contents of β-structure of the fusion peptides in lipid bilayers and that this increase correlated with an inhibition of membrane fusion (*8*).

Effects of the influenza virus fusion peptides on the structure of the lipid bilayer have also been studied by several groups. For example, Colotto and Epand (*13*) observed that the formation of cubic lipid phases is promoted by the presence of the fusion peptide at pH 5. Gray et al. (*8*) found that a longer version of this fusion peptide induced an increase of the order parameter of the lipid hydrocarbon chains, and that mutant peptides with fusion-inhibiting amino acid replacements in the amino-terminal position altered the hydrogen bonding pattern in the lipid polar headgroup region.

The focus of the work presented here is the structural role of two alanine residues and one glycine residue in positions 5, 7, and 8, respectively, i.e., about one-third into the fusion peptide region. These residues are totally conserved in all influenza hemagglutinin sequences which suggests that they perform an important structural and/or functional role. Therefore, we introduced several mutations in these positions and studied the fusion activity of expressed HAs and the conformations and orientations of the corresponding synthetic peptides in lipid bilayers. By simply changing the hydrophobic volume of these residues (alanines to glycines and valines), we attempted to probe whether structural changes due to hydrophobic packing constraints in lipid bilayers could explain the fusion behavior of each of these constructs. Some, but not all, of the introduced hydrophobic fusion peptide mutations significantly decreased the level of membrane fusion. Despite their different fusion behavior, all peptides were predominantly α-helical in lipid bilayers and contained minor levels of β-structure. No significant difference in the oblique orientation relative to the lipid bilayer was observed between the fusogenic and nonfusogenic peptides. The order parameters of lipid hydrocarbon chains were increased to a greater extent in the presence of the fusogenic than in the presence of the nonfusogenic peptides.

MATERIALS AND METHODS

Peptides and Lipids. Twenty-three-residue peptides with unblocked N- and C-termini were made by the F-moc procedure (*14*) on an Applied Biosystems 430A peptide synthesizer. They were precipitated three times from diethyl ether; mass spectrometry was used to check for correct composition, and high-performance liquid chromatography showed the peptides to be >95% pure. DMPC was purchased from Avanti Polar Lipids (Alabaster, AL) and used without further purification.

Mutagenesis and Expression of Hemagglutinins. Site-specific mutagenesis was carried out by the method of Kunkel et al. (*15*). Wild-type and mutant hemagglutinins were expressed in BHK21 cells as described by Steinhauer et al. (*12*) using the 7.5 K early-late promoter and the Copenhagen strain of vaccinia virus. Cell surface expression was assessed by ELISA as described previously (*12*). All values are averages from three or five independent experiments.

Heterokaryon Fusion Assay. HA-expressing BHK21 cells (15 h postinfection) were treated with 5 μg/mL trypsin for 5 min at 37 °C to cleave the HA_0 to HA_1 and HA_2 and then with trypsin inhibitor (5 μg/mL). The cells were then incubated at pH 5 for 1 min and subsequently overlaid with DMEM containing fetal calf serum for 1 h. Cells were fixed in 2.5% (v/v) glutaraldehyde for 15 min and stained with 1% (w/v) toluidine blue.

Hemolysis Experiments. Peptide (2.5 μg from a stock of 5 mg/mL peptide in DMSO) was incubated with 0.5 mL of washed human erythrocytes (2% hematocrit in PBS). After the pH had been lowered to 5 with an aliquot of 0.15 M citrate buffer (pH 3.5), the mixture was incubated at 37 °C for 45 min. Cells were pelleted at 3000*g* for 1 min, and the OD of the supernatant was determined at 520 nm. Complete hemolysis was obtained after lysing the cells with 0.5% Brij 36T.

Preparation of Lipid Vesicles. DMPC (1.0 μmol) in chloroform was mixed with an appropriate volume of peptide dissolved in DMSO to obtain the desired peptide-to-lipid ratio. The solvent was evaporated under a stream of nitrogen; the dried lipid/peptide mixture was subjected to a high vacuum overnight to remove trace amounts of solvent, and 1.0 mL of pH 7.4 buffer [5 mM HEPES, 10 mM MES, and 150 mM NaCl (pH 7.4)] was added. Small unilamellar vesicles to be used for CD spectroscopy were prepared by sonicating the lipid/peptide dispersions with a Branson tip probe sonicator for 30 min at 50% duty cycle in an ice bath. Titanium dust was removed by centrifugation. For measurements at pH 5, a buffer consisting of 5 mM HEPES, 10 mM MES, and 150 mM NaCl (pH 5.0) was used instead of the pH 7.4 buffer. Large unilamellar vesicles to be used for the preparation of planar-supported bilayers and subsequent ATR-FTIR experiments were prepared by extrusion through polycarbonate membranes. After five freeze−thaw cycles, the lipid suspension was extruded 15 times through two stacked polycarbonate membranes (100 nm pore size; Nucleopore, Pleasanton, CA) using the "Liposofast" extruder (Avestin, Ottawa, ON).

Preparation of Supported Bilayers. Planar phospholipid bilayers supported on germanium ATR plates were prepared as previously described (*16*). Briefly, a monomolecular film of DMPC dissolved in 9:1 (v/v) hexane/ethanol was spread at low pressure onto an aqueous buffer [10 mM Tris/acetic acid (pH 5.0)] in a Langmuir-Blodgett trough (Nima model 611, Coventry, England). The monolayer was compressed to 32 mN/m. The germanium plate (50 mm × 20 mm × 1 mm with 45° beveled edges; Spectral Systems, Irvington, NY) was carefully cleaned with ethanol, methanol, and hexane in sequence. After further cleaning in an Ar plasma cleaner (Harrick, Ossining, NY) for 10 min, the plate was vertically immersed through the monolayer at a rate of 50 mm/min and slowly withdrawn at a rate of 2 mm/min. The surface pressure of the monolayer was held constant at 32 mN/m during the coating procedure. The plate was assembled in the measuring cell, and extruded vesicles with or without incorporated peptide were injected into the cell and incubated at room temperature for 3 h, yielding a single supported bilayer on both sides of the germanium plate. Excess unfused vesicles and unbound peptides were removed by flushing the cell with 6 mL (approximately 8 cell volumes) of D_2O buffer (5 mM HEPES, 10 mM MES, and 150 mM NaCl in D_2O, with the pH adjusted to 7.4 or 5.0 with NaOH).

CD Spectroscopy. Circular dichroism spectra were recorded on a Jasco 700 CD spectrometer (Jasco, Rochester, NY). The spectra were measured at a peptide concentration

of 0.3 mM and a peptide-to-lipid molar ratio of 1:10 in a 0.1 mm path length cell at room temperature. The actual concentration of each sample was determined by measuring the absorbance at 285 nm of a small aliquot that was diluted into DMSO and calibrating the measured value with a peptide standard in DMSO. The concentration of the standard was determined by quantitative amino acid analysis. Each spectrum was obtained by averaging five scans that were recorded at a rate of 10 nm/min between 190 and 250 nm. The CD spectra were corrected for signal arising from sources other than peptide by subtracting spectra obtained with vesicles with the identical composition and concentration, but without peptide. Some spectra were also recorded at 30 °C, but no difference was found.

FTIR Spectroscopy. Polarized ATR-FTIR spectra of supported bilayers were recorded on a Nicolet 740 Fourier transform infrared spectrometer at room temperature as described previously (*17*). The instrument was purged with nitrogen for 2 h to remove H_2O vapor. Two thousand scans were co-added each at parallel and perpendicular polarization and at pH 7.4 and 5.0 with a nominal resolution of 2 cm^{-1}. ATR spectra of D_2O buffers at the respective pH and orientation of polarization were used as references for converting transmittance to absorbance spectra. The methods of processing and calculations of order parameters, defined as

$$S = \frac{3\langle \cos^2 \theta \rangle - 1}{2} \quad (1)$$

where θ is the angle of the individual molecular orientations from the membrane normal in the ensemble, were as described previously (*8*, *18*). Briefly, order parameters reflecting the order of the lipid acyl chains were calculated from the ATR dichroic ratios ($R^{ATR} = A_{\parallel}/A_{\perp}$) of the methylene stretching bands according to

$$S_L = -2\frac{E_x^2 - R^{ATR}E_y^2 + E_z^2}{E_x^2 - R^{ATR}E_y^2 - 2E_z^2} \quad (2)$$

and order parameters reflecting the orientational distribution of the helical segments of the peptides in the lipid bilayer were calculated from the ATR dichroic ratios of the amide I′ band component at 1650−1658 cm^{-1} according to

$$S_H = (1/f_H)\left(\frac{2}{3\cos^2 \alpha - 1}\right)\left(\frac{E_x^2 - R^{ATR}E_y^2 + E_z^2}{E_x^2 - R^{ATR}E_y^2 - 2E_z^2}\right) \quad (3)$$

Since the fusion peptides are mostly inserted into the lipid bilayer, the thin-film approximation was used for calculation of the electric field components which were as follows under the conditions that were used: $E_x^2 = 1.969$, $E_y^2 = 2.249$, and $E_z^2 = 1.892$ (*18*). The angle α is the angle between the amide I transition moment and the helix axis and is 39° (*18*). The parameter f_H is the fraction of residues in an α-helical conformation that contributes to the band component at 1650−1658 cm^{-1}.

RESULTS

Expression and Fusion Activity of Mutant HA Molecules. The sequence of the fusion peptide of influenza strain X:31 hemagglutinin reads GLFG**A**I**AG**FIENGWEGMIDGWYG. HA glycoproteins with single-site mutations in the fusion peptide region were expressed in BHK21 cells using the vaccinia system as described in Materials and Methods. Specifically, the alanines in positions 5 and 7 were changed to glycines and valines, and glycine 8 was changed to an alanine. These mutations were designed to change the hydrophobic volumes of the residues in question. ELISA experiments with nonpermeabilized cells showed that all the HAs were expressed to similar extents on the cell surface. Expression levels were 100% for the wild type, 94% for A5G, 128% for A5V, 94% for A7G, 106% for A7V, and 104% for G8A. All HAs could be cleaved by trypsin into HA_1 and HA_2 and could undergo a conformational change at low pH as judged by an assay in which the release of HA_1 by 20 mM dithiothreitol is monitored (*19*) (results not shown). Figure 1 shows the fusion activity of the mutant HA molecules using a heterokaryon formation assay. Cells expressing wild-type, A5G, and A7V HAs all formed heterokarya after incubation at pH 5 for 1 min at 37 °C. Fusion activity was inhibited between cells expressing A5V or A7G HAs. It has previously been reported that cells expressing G8A HA exhibited very little fusion activity (*12*). These results show that introducing mutations toward the center of the fusion peptide has significant effects upon the fusion properties of the HA molecules (Table 1).

Hemolysis Activity of Synthetic Fusion Peptide Mutants. To use synthetic peptides as a valid model system for biophysical studies of the fusion peptide region, it is important that the peptides interact with the lipid bilayer in a manner similar to that of the fusion peptide region of the full-length HA molecules. Hemolysis was used to study the fusion properties of the fusion peptides. Experiments with virus, isolated HA rosettes, and fusion peptides have shown that hemolytic activity correlates with membrane fusion activity (*11*, *20*, *21*). Table 1 shows the hemolysis caused by incubation of red blood cells with the various peptides at pH 5. None of the peptides caused hemolysis at pH 7 (results not shown). To provide for a single tryptophan in the 23-residue sequences, tryptophan 21 was replaced with a phenylalanine in all the peptides used in this study. This relatively conservative change did not affect the hemolytic activity of these peptides. The A5G and A7V peptides had activities similar to that of wild type; the G8A peptide had a decreased level of hemolysis, whereas the A5V and A7G peptides exhibited levels of hemolysis similar to background. Therefore, the degree of hemolysis activity of the peptides closely matches the fusion activity of the intact HA glycoproteins, the only difference being that the G8A HA exhibited no fusion activity while the corresponding peptide exhibited a small amount of hemolysis. We also synthesized peptides with mutations at both the 5 and 7 positions. When these residues were mutated to valines (A5V/A7V) or glycines (A5G/A7G), the hemolysis activity of the peptides was greatly decreased.

Secondary Structure of the Fusion Peptides in Lipid Bilayers. Far-UV CD spectra of the peptides bound to small unilamellar vesicles of DMPC at pH 7.4 are shown in Figure 2. The spectra of the fusion-active peptides are grouped in panel A and those of the fusion-inactive peptides in panel B. Very similar spectra were obtained at pH 5. The fraction of residues in an α-helical conformation was calculated for each peptide from the ratio of the experimental mean residue

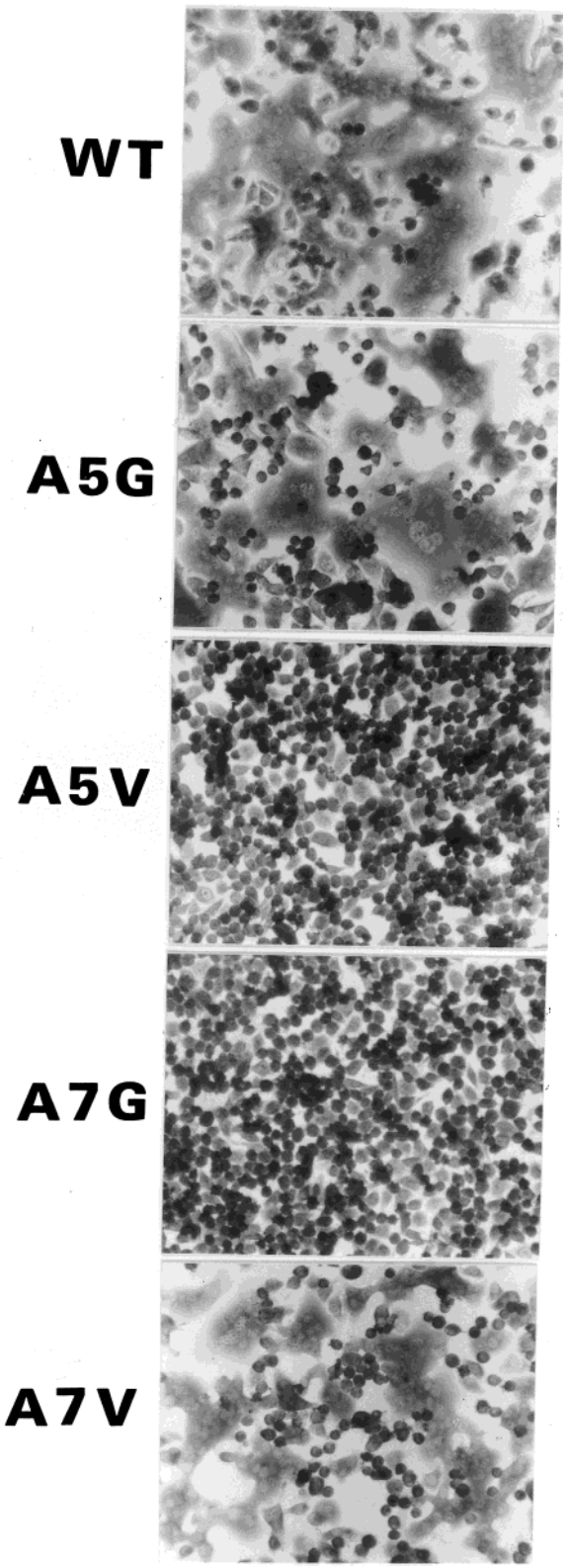

FIGURE 1: Heterokaryon formation by BHK21 cells expressing wild-type or mutant HA. The wild type and the fusion peptide mutants A5G and A7V form heterokarya after incubation for 1 min at pH 5, whereas the mutant HAs with the A5V and A7G substitutions do not form heterokarya under otherwise identical conditions.

molar ellipticity at 222 nm to a molar ellipticity of -30×10^3 deg cm^2 dmol^{-1} which was taken to represent 100% helical secondary structure (*22*). As shown in Table 1, the average helicities ranged from 25 to 50% at pH 7.4 and from 31 to 47% at pH 5. Apart from one possible exception (A5G/A7G), the helicities of the peptides varied by less than 10% when the pH was changed from 7.4 to 5. A 10% change is within the range of experimental error of these measurements which is mainly determined by uncertainties of the absolute peptide concentrations in each sample. Therefore, the helicities of these peptides (except that of A5G/A7G) do not appear to depend on pH. Of all peptides used in this study, G8A appears to be the most helical and the two double mutants appear to be the least helical.

Table 1: Fusion and Hemolysis Activities and Percent α-Helix in DMPC Bilayers of Wild-Type and Mutant HA Fusion Peptides

peptide	heterokaryon formation[a]	hemolysis (%)[b]	α-helix (%)[c]	
			pH 7.4	pH 5.0
wild type	+	81	42	37
A5G	+	92	36	42
A7V	+	74	45	36
A5V	−	2	34	43
A7G	−	1	39	33
A5G/A7G	nd[d]	6	46	31
A5V/A7V	nd	1	25	31
G8A	−	32	50	47

[a] Measured between cells expressing HAs with the respective mutations at pH 5. [b] Measured with synthetic peptides at pH 5. [c] Estimated from CD spectra of synthetic peptides bound to lipid bilayers. [d] Not determined.

Polarized ATR-FTIR spectra in the amide I′ region are shown in Figure 3 for the wild-type, A5V, A5G, A7V, and A7G peptides in supported bilayers of DMPC at pH 7.4. The amide I′ bands of all peptides exhibited multiple components which allowed us to determine the relative amounts of β-structure of these peptides. The amide I′ bands of peptides G8A, A5G/A7G, and A5V/A7V were too weak to allow for a reliable quantitation of secondary structure. Decomposition of the amide I′ bands of the five peptides whose results are depicted in Figure 3 consistently yielded three distinct Gaussian component bands centered at 1676−1682, 1650−1658, and 1628−1630 cm^{-1}. The calculated summed spectra of these three components reproduced the experimental amide I′ contours very well. The first component is attributed to residues in turn structures and may also contain the weak high-frequency counterpart that is usually present in spectra of antiparallel β-sheets. The second component arises from α-helices and irregular secondary structures, and the third component represents residues in a β-strand conformation. The relative band areas are listed in Table 2. The relative levels of β-structure in these peptides were calculated from the area fractions of the component at 1629 cm^{-1} and by taking into account the fact that the molar (integrated) extinction coefficient of this component is about 1.4 times larger than those of the other components (*23*, *24*). The percentages of β-structure of the fusion peptides range from 13 to 16% and are also listed in Table 2. Lowering the pH to 5 had no significant effect on the relative levels of β-structure in these peptides.

Orientation of Fusion Peptides in Lipid Bilayers. The order parameters representing the helix orientation of the five peptides whose results are depicted in Figure 3 were determined from the linear dichroism of the ATR-FTIR α-helical amide I′ band. An important parameter that enters the calculation of helical order parameters from the ATR dichroic ratio, R_{1655}^{ATR}, is the fraction of helical residues

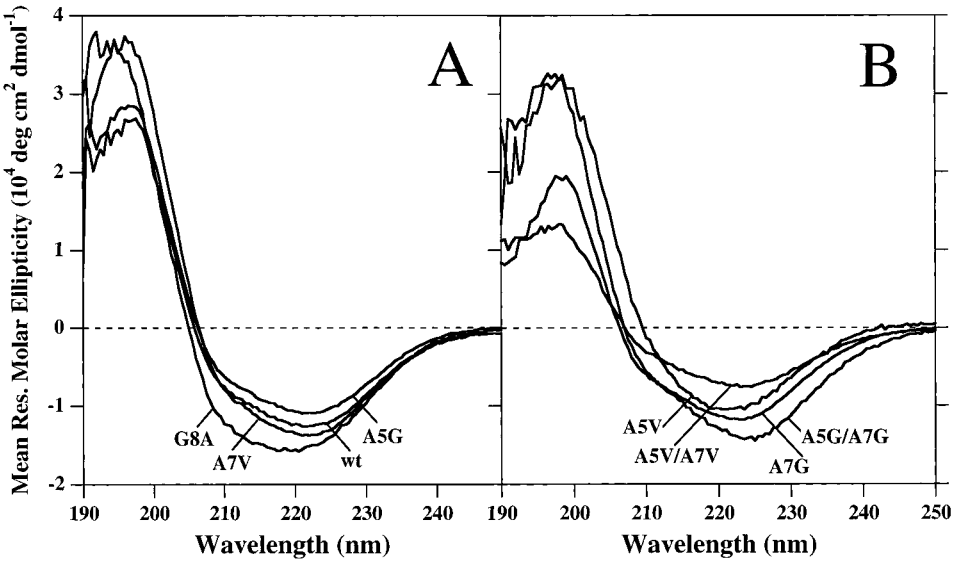

FIGURE 2: CD spectra of the fusogenic wild-type, A5G, and A7V peptides and the partially fusogenic peptide G8A (A) and the nonfusogenic peptides A5V, A7G, A5G/A7G, and A6V/A7V (B) bound to small unilamellar vesicles of DMPC at pH 7.4 and measured at room temperature. Similar spectra were obtained at pH 5.

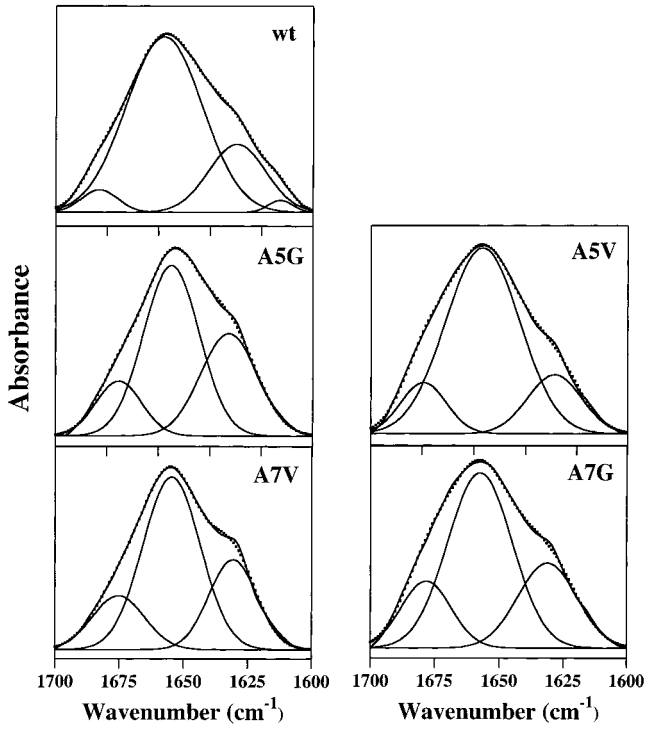

FIGURE 3: Parallel polarized ATR-FTIR spectra in the amide I′ region of the fusogenic wild-type, A5G, and A7V peptides (left column) and the nonfusogenic peptides A5V and A7G (right column) bound to supported bilayers of DMPC at pH 7.4. All spectra were decomposed into three (or four) Gaussian components centered at approximately 1680, 1655, and 1629 cm^{-1} (1613 cm^{-1}). The dotted lines are the sums of the curve-fitted component bands. The spectra were recorded at room temperature. Similar spectra were obtained at pH 5.

Table 2: Fractional Areas and Percent β-Structure of the Wild-Type and Mutant Fusion Peptides As Determined from the Amide I′ Band Components of the FTIR Spectra of Figure 3

peptide[a]	1680 cm^{-1}	1655 cm^{-1}	1629 cm^{-1}	β-structure (%)[b]
wild type (+)	4	78	18	14
A5G (+)	11	68	21	16
A7V (+)	8	72	20	15
A5V (−)	10	73	17	13
A7G (−)	8	72	20	15

[a] The + and − signs in parentheses indicate the fusogenicity of each peptide. [b] Calculated from the band area at 1629 cm^{-1} taking into account the fact that the extinction coefficient of this band is about 1.4 times larger than those of the other bands.

Table 3: Dichroic Ratios, Helical Order Parameters, and "Average" Angles from the Membrane Normal of the Helical Segments of the Wild-Type and Mutant Fusion Peptides

peptide[a]		R_{1655}^{ATR}	f_H[b]	S_H	θ[c]
wild type (+)	pH 7.4	2.2 ± 0.2	0.53	$0.59^{+0.26}_{-0.22}$	32
	pH 5.0	2.2 ± 0.2	0.49	$0.64^{+0.28}_{-0.24}$	29
A5G (+)	pH 7.4	1.8 ± 0.2	0.53	$0.12^{+0.25}_{-0.29}$	50
	pH 5.0	1.7 ± 0.1	0.55	$-0.02^{+0.13}_{-0.15}$	55
A7V (+)	pH 7.4	2.0 ± 0.2	0.60	$0.33^{+0.19}_{-0.23}$	42
	pH 5.0	2.0 ± 0.3	0.45	$0.44^{+0.39}_{-0.48}$	38
A5V (−)	pH 7.4	1.8 ± 0.1	0.46	$0.14^{+0.15}_{-0.16}$	49
	pH 5.0	1.9 ± 0.2	0.59	$0.23^{+0.20}_{-0.24}$	46
A7G (−)	pH 7.4	1.9 ± 0.1	0.57	$0.23^{+0.14}_{-0.12}$	46
	pH 5.0	1.9 ± 0.1	0.43	$0.31^{+0.15}_{-0.16}$	43

[a] The + and − signs in parentheses indicate the fusogenicity of each peptide. [b] Ratio of residues in an α-helical conformation divided by the sum of residues in an α-helical and irregular conformation. [c] "Average" angle of the α-helical axis of the peptide to the membrane normal, calculated from S_H assuming unique orientations.

contributing to the amide I′ band component at 1650−1658 cm^{-1}, f_H. Consideration of this parameter is important because there is a significant contribution from irregular structures to this component. Since it is difficult to distinguish between α-helical and irregular secondary structure by FTIR spectroscopy (*18*), we took the number of α-helical residues in each peptide from the CD data of Table 1 and calculated f_H by dividing by the sum of the number of residues in α-helical and irregular conformations as determined from the FTIR band component at 1655 cm^{-1} (Table 2). These results are presented in Table 3. The average helical order parameters, S_H, range from 0.0 to 0.6 which correspond to angles from 30 to 55° to the membrane normal, if in a given sample all peptides were aligned at the same angle. (A wider

Table 4: Dichroic Ratios and Derived Order Parameters of the Lipid Methylene Stretching Vibrations Measured from Polarized ATR-FTIR Spectra of Wild-Type and Mutant Fusion Peptides in Supported DMPC Bilayers[a]

	2852 cm^{-1} [c]				2924 cm^{-1} [d]			
	pH 7.4		pH 5.0		pH 7.4		pH 5.0	
peptide[b]	R^{ATR}	S_L	R^{ATR}	S_L	R^{ATR}	S_L	R^{ATR}	S_L
−[e]	1.47 ± 0.03	0.21 ± 0.03	1.36 ± 0.05	0.33 ± 0.05	1.52 ± 0.02	0.17 ± 0.02	1.43 ± 0.03	0.26 ± 0.03
wild type (+)	1.15 ± 0.03	0.58 ± 0.05	1.08 ± 0.02	0.67 ± 0.03	1.21 ± 0.02	0.51 ± 0.03	1.15 ± 0.03	0.58 ± 0.04
A5G (+)	1.16 ± 0.06	0.57 ± 0.07	1.25 ± 0.06	0.46 ± 0.07	1.23 ± 0.01	0.47 ± 0.01	1.29 ± 0.06	0.42 ± 0.07
A7V (+)	1.09 ± 0.01	0.67 ± 0.02	1.15 ± 0.05	0.59 ± 0.07	1.21 ± 0.05	0.50 ± 0.06	1.19 ± 0.04	0.53 ± 0.05
A7G (−)	1.35 ± 0.05	0.35 ± 0.05	1.30 ± 0.04	0.39 ± 0.04	1.36 ± 0.08	0.33 ± 0.08	1.38 ± 0.07	0.30 ± 0.07
A5V (−)	1.34 ± 0.06	0.35 ± 0.06	1.33 ± 0.04	0.36 ± 0.05	1.33 ± 0.03	0.35 ± 0.02	1.37 ± 0.01	0.33 ± 0.03
A5G/A7G (−)	1.23 ± 0.05	0.48 ± 0.06	1.28 ± 0.04	0.42 ± 0.05	1.29 ± 0.06	0.41 ± 0.09	1.30 ± 0.06	0.39 ± 0.07
A5V/A7V (−)	1.36 ± 0.03	0.34 ± 0.03	1.39 ± 0.01	0.30 ± 0.02	1.41 ± 0.05	0.28 ± 0.05	1.45 ± 0.05	0.25 ± 0.05
G8A (30%)	1.12 ± 0.01	0.63 ± 0.01	1.14 ± 0.01	0.60 ± 0.02	1.18 ± 0.02	0.54 ± 0.03	1.18 ± 0.02	0.53 ± 0.04

[a] Data are averages of three independent measurements for each peptide. [b] The + and − signs in parentheses indicate the fusogenicity of each peptide. G8A is about 30% fusogenic. [c] Symmetric CH_2 stretch. [d] Asymmetric CH_2 stretch. [e] Pure DMPC bilayer. No peptide added.

range of angles would account for the experimental data if angular distributions instead of unique orientations were used to interpret the measured order parameters. See eq 1 for a definition of order parameters.) Clearly, all five peptides inserted into DMPC bilayers at oblique angles from the membrane normal. This oblique orientation did not depend on the pH of the environment.

Effect of Fusion Peptides on Lipid Order. As a measure of the order of the lipid hydrocarbon chains in supported bilayers, the dichroic ratios of the methylene stretching vibrations at 2924 and 2852 cm^{-1} were determined from the polarized ATR-FTIR spectra. These values and the corresponding order parameters of the bands at 2852 and 2924 cm^{-1} are listed in Table 4. The order parameters calculated from both bands fall into two categories which correlate with the fusogenicities of the fusion peptides. In a first group that comprises all measurements that were performed in the presence of the fusogenic peptides, the order parameters derived from the symmetric CH_2 stretching bands at 2852 cm^{-1} range from 0.55 to 0.7. (A single exception was the A5G peptide which exhibited an order parameter of 0.46 at pH 5, but 0.57 at pH 7.4.) In marked contrast, when these lipid order parameters were measured in the presence of the nonfusogenic peptides, values that range from 0.3 to 0.4 were found. (A single exception was the A5G/A7G peptide which had order parameters of 0.48 and 0.42 at pH 7.4 and 5, respectively.) Thus, a trend exists which indicates that the lipid order parameters are generally larger for the fusogenic than for the nonfusogenic peptides (Figure 4). Analysis of the order parameters derived from the antisymmetric CH_2 stretching bands at 2924 cm^{-1} produced a very similar graph (data shown in Table 4 only) and, therefore, lead to the same general conclusion. In summary, these results suggest that the hydrocarbon chains in the lipid bilayer become more ordered in the presence of the fusogenic peptides, but are affected little by the nonfusogenic peptides. The pH of the environment has no significant effect on the lipid ordering behavior of the fusogenic peptides.

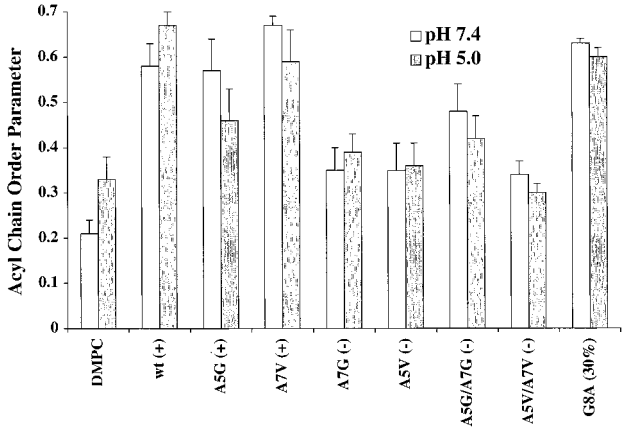

FIGURE 4: Order parameters determined from the ATR dichroic ratios of the DMPC methylene symmetric stretching vibrations at 2852 cm^{-1} of wild-type and mutant fusion peptides at pH 7.4 and 5. The + and − signs in parentheses indicate the fusogenicity of each peptide.

DISCUSSION

Although it has long been known that the fusion peptide plays a crucial role in viral membrane fusion by interacting with the lipid bilayer of the target membrane, its precise structure in lipid bilayers is not known. Yet, the sequence of the fusion peptide is one of the most conserved regions of the viral envelope glycoproteins that mediate membrane fusion. Therefore, the structure of the fusion peptide in lipid bilayers is doubtless very important for membrane fusion. Our approach to uncovering structure−function relationships in the fusion peptide region of the influenza virus HA is to perturb the sequence of this peptide by relatively gentle yet functionally effective mutations and to find correlations between function and structural changes and modified interactions of these peptides with lipid bilayers. Previous studies using this approach have focused on the extreme N-terminus of the fusion pepitde. It has been known for a quite some time that the N-terminal glycine residue is important for fusion. Fusion is completely abolished when this residue is deleted (*11*, *12*, *25*) or changed to a glutamate (*10*). Replacements of Gly-1 with Phe, His, Ile, Leu, or Ser or inserting an additional Ala after Gly-1 also blocks fusion, whereas replacing it with an Ala or appending an additional Ala before Gly-1 is tolerated (*12*). More recently, Qiao et al. (*26*) showed that the phenotype of the Ser mutant in this position actually is a hemifusion mutant in which only the proximal but not the distal leaflets of the lipid bilayer are merged. It is also reported in this latter study that Val, Glu, Gln, and Lys replacements for Gly-1 are completely fusion-inactive. Biophysical studies with peptides corresponding to the deletion, Glu replacement, and Ala insertion mutants at the N-terminus show that these peptides exhibit higher levels

of β-structure and lower levels of α-helix compared to the wild-type peptide when these peptides are inserted into lipid bilayers (*8*). In contrast to the wild-type peptide, these mutant fusion peptides also break hydrogen bonds between lipid ester carbonyls and water either directly by interaction of the mutated residues or indirectly by the increased β-strand propensity of the mutant peptides.

Several residues within the fusion peptide, namely, Leu-2, Phe-3, Gly-4, Ile-6, Phe-9, Glu-11, and Glu-15, are less sensitive to moderate mutations (*12*). In contrast, Ala-5, Ala-7, and Gly-8 are highly conserved and no permissive mutations were identified in these positions prior to this study. Therefore, we suspected that these residues could be particularly important for fusion and that changes in these positions might alter the structure and interactions of these peptides in lipid bilayers. A first step in our attempt to establish structure−function relationships for these residues was to introduce a few conservative mutations in these positions. To decrease and increase the hydrophobic volumes of these residues, we changed the alanines to glycines and valines, respectively, which can be considered very moderate changes. Interestingly, a smaller but not a larger residue was tolerated in position 5, whereas the converse was true for position 7 (Figure 1 and Table 1). When Gly-8 was replaced with an alanine, fusion was inhibited (*12*) and the corresponding peptide was only marginally hemolytic (Table 1). Double mutations in positions 5 and 7 also lead to inactive fusion peptides. These results confirm that the three conserved residues in positions 5, 7, and 8 are extremely sensitive to only subtle mutations.

Although valines have a slightly higher propensity for α-helix in membranes than alanines (*27*), we did not observe a significant increase in helicity in the Ala-to-Val mutant peptides (Table 1). (The double valine mutant was actually slightly less helical than the wild-type peptide.) Glycines tend to disrupt helices in globular proteins or peptides in solution (*28*), but still support helix formation in membrane environments (*27*). Consistent with this expectation, we did not observe significant changes in helicity in our Ala-to-Gly mutant peptides. The marginally hemolytic Gly-to-Ala peptide exhibited a slightly increased helicity compared to the wild type. When these results and our previous results on the N-terminally mutated peptides (*8*) are taken together, it appears that "successful" fusion peptides are about 40% α-helical based on peptides that include the first 23 residues of strain X:31 HA2. Significant deviations from this value (up or down) appear not to be conducive to fusion. However, it is also clear from the studies presented here that although necessary, the requirement for ∼40% helix is not sufficient to make an active fusion peptide. In addition to α-helix, small amounts of β-structure (13−16%) are also present in all the peptides used in this study. However, and in contrast to the N-terminally mutated peptides (*8*), the fraction of β-structure does not discriminate between fusogenic and nonfusogenic species of the peptides with internal mutations studied here (Table 2).

It has been argued often that an insertion of the α-helix at an oblique angle is characteristic for fusion peptides in lipid bilayers (*4*, *6*−*9*). These polarized FTIR measurements again support this general conclusion (Table 3). However, no discrimination between fusogenic and nonfusogenic peptides was evident from these measurements. Both classes of peptides inserted at oblique angles, i.e., roughly 30−55° from the membrane normal. Although we did not observe a correlation between order parameter (insertion angle) and fusogenicity, small angular differences between the two classes of peptides cannot be excluded because the standard errors of our dichroic ratios are relatively large. The reason for the magnitude of these errors is that these measurements were conducted on single supported bilayers rather than multibilayer samples that are often used by other investigators. However, we think that it is very important to use fully hydrated bilayers as was done in our studies, because conformations and orientations of amphiphilic peptides can be very sensitive to the degree of hydration of the host lipid bilayer. Partially hydrated stacks of interacting bilayers are probably not adequate for meaningful studies of peptide conformation and their interactions with lipids in these systems (*18*, *29*).

In this work, we found that most fusogenic peptides increased the packing order of the lipid acyl chains whereas the nonfusogenic peptides did not (Figure 4). Supported lipid bilayers of DMPC are fluid at 21−22 °C (*30*) and exhibit an acyl chain order parameter of 0.3−0.4 (*18*). The nonfusogenic peptides at a peptide-to-lipid molar ratio of 1:10 did not noticeably alter this order parameter, except for A5G/A7G whose order parameter moderately increased to 0.48 at pH 7.4. However, the fusogenic peptides increased this order parameter to 0.55−0.7, except for A5G which exhibited only a moderate increase to 0.46 at pH 5. (At pH 7.4, the increase to 0.57 was as large as expected for the fusogenic peptides.) An increase in the order parameter would be expected if the bilayers were partially dehydrated at the surface by the action of the peptide because surface hydration and chain order are known to be coupled in lipid bilayers (*31*−*33*). The possibility that (active) fusion peptides could partially dehydrate membrane surfaces is interesting because it is clear that repulsive hydration forces must be overcome to allow membranes to fuse (*34*, *35*). Therefore, the fusion peptides could promote fusion not only by altering lipid curvature as previously proposed (*13*) but also by dehydrating membrane surfaces and thus making them more hydrophobic than unperturbed lipid bilayers. This proposal in the context of viral fusion proteins is particularly interesting because we recently discovered that the helical transmembrane domain of influenza hemagglutinin exerts a similar effect on the lipids in model lipid bilayers and thus, presumably, also in viral membranes (*36*). Therefore, an appealing mechanism for viral spike glycoprotein-mediated fusion would include an increase in the viral and target membrane surface hydrophobicities as prerequisites for fusion. In this model, insertion of the fusion peptide would be preceded by the "spring-loaded" coiled coil transitions of the soluble part of the fusion protein (*37*, *38*) and the fusion foci of the two membranes would be brought into close contact by the concerted tilting of the coiled coils in the fusion site as experimentally observed by ATR-FTIR spectroscopy (*39*−*41*).

In conclusion, gentle mutations at the most conserved sites of the influenza hemagglutinin fusion peptide do not appreciably alter the secondary structure and orientation of these peptides in lipid bilayers, although they can abolish the fusion activity of the parent fusion proteins. Rather than by subtle conformational change, they appear to compromise

membrane fusion by altering the packing order of the lipid bilayers into which they insert and, as a possible consequence, by altering the surface hydrophobicity of the membranes to be fused.

ACKNOWLEDGMENT

We thank Peter Fletcher for synthesis of peptides and Carol Newman for assistance with the vaccinia expression studies.

REFERENCES

1. Murata, M., Sugahara, Y., Takahashi, S., and Ohnishi, S.-I. (1987) *J. Biochem. 102*, 957−962.
2. Lear, J. D., and DeGrado, W. F. (1987) *J. Biol. Chem. 262*, 6500−6505.
3. Takahashi, S. (1990) *Biochemistry 29*, 6257−6264.
4. Brasseur, R., Vandenbranden, M., Cornet, B., Burny, A., and Ruysschaert, J. (1990) *Biochim. Biophys. Acta 1029*, 267−273.
5. Rafalski, M., Ortiz, A., Rockwell, A., van Ginkel, L. C., Lear, J. D., DeGrado, W. F., and Wilschut, J. (1991) *Biochemistry 30*, 10211−10220.
6. Ishiguro, R., Kimura, N., and Takahashi, S. (1993) *Biochemistry 32*, 9792−9797.
7. Lüneberg, J., Martin, I., Nüssler, F., Ruysschaert, J.-M., and Herrmann, A. (1995) *J. Biol. Chem. 270*, 27606−27614.
8. Gray, C., Tatulian, S. A., Wharton, S. A., and Tamm, L. K. (1996) *Biophys. J. 70*, 2275−2286.
9. Macosko, J. C., Kim, C.-H., and Shin, Y.-K. (1997) *J. Mol. Biol. 267*, 1139−1148.
10. Gething, M. J., Doms, R. W., York, D., and White, J. (1986) *J. Cell Biol. 102*, 11−23.
11. Wharton, S. A., Martin, S. R., Ruigrok, R. W. H., Skehel, J. J., and Wiley, D. C. (1988) *J. Gen. Virol. 69*, 1847−1857.
12. Steinhauer, D. A., Wharton, S. A., Skehel, J. J., and Wiley, D. C. (1995) *J. Virol. 69*, 6643−6651.
13. Colotto, A., and Epand, R. M. (1997) *Biochemistry 36*, 7644−7651.
14. Atherton, E., and Sheppard, R. C. (1985) *J. Chem. Soc., Chem. Commun.*, 165−166.
15. Kunkel, T. A., Roberts, J. D., and Zakour, R. A. (1987) *Methods Enzymol. 154*, 367−382.
16. Frey, S., and Tamm, L. K. (1991) *Biophys. J. 60*, 922−930.
17. Tamm, L. K., and Tatulian, S. A. (1993) *Biochemistry 32*, 7720−7726.
18. Tamm, L. K., and Tatulian, S. A. (1997) *Q. Rev. Biophys. 30*, 365−429.
19. Graves, P. N., Schulman, J. F., Young, J. F., and Palese, P. (1983) *Virology 126*, 106−116.
20. Sato, S. B., Kawasaki, K., and Ohnishi, S.-I. (1983) *Proc. Natl. Acad. Sci. U.S.A. 80*, 3153−3157.
21. Wharton, S. A., Skehel, J. J., and Wiley, D. C. (1986) *Virology 149*, 27−35.
22. Yang, J. T., Wu, C.-S. C., and Martinez, H. M. (1986) *Methods Enzymol. 130*, 208−269.
23. Chirgadze, Yu. N., Shestopalov, B. V., and Yu, S. (1973) *Biopolymers 12*, 1337−1351.
24. Chirgadze, Yu. N., and Brazhnikov, E. V. (1974) *Biopolymers 13*, 1701−1712.
25. Garten, W., Bosch, F. X., Linder, D., Rott, R., and Klenk, H. D. (1981) *Virology 115*, 361−374.
26. Qiao, H., Armstrong, R. T., Melikyan, G. B., Cohen, F. S., and White, J. M. (1999) *Mol. Biol. Cell 10*, 2759−2769.
27. Li, S. C., and Deber, C. M. (1994) *Nat. Struct. Biol. 1*, 368−373.
28. Chou, P. Y., and Fasman, G. D. (1978) *Annu. Rev. Biochem. 47*, 251−276.
29. Silvestro, L., and Axelsen, P. H. (1998) *Chem. Phys. Lipids 96*, 69−80.
30. Tamm, L. K. (1988) *Biochemistry 27*, 1450−1457.
31. Lis, L. J., McAlister, M., and Rand, R. P. (1982) *Biophys. J. 37*, 657−666.
32. Evans, E. A., and Parsegian, V. A. (1986) *Proc. Natl. Acad. Sci. U.S.A. 83*, 7132−7136.
33. Gawrisch, K., Ruston, D., Zimmerberg, J., Parsegian, V. A., Rand, R. P., and Fuller, N. (1992) *Biophys. J. 61*, 1213−1223.
34. McIntosh, T. J., and Simon, S. A. (1994) *Annu. Rev. Biophys. Biomol. Struct. 23*, 27−51.
35. Leckband, D. E., Helm, C. A., and Israelachvili, J. (1993) *Biochemistry 32*, 1127−1140.
36. Tatulian, S. A., and Tamm, L. K. (1999) *Biochemistry* (submitted for publication).
37. Carr, C. M., and Kim, P. S. (1993) *Cell 73*, 823−832.
38. Bullough, P. A., Hughson, F. M., Skehel, J. J., and Wiley, D. C. (1994) *Nature 371*, 37−43.
39. Tatulian, S. A., Hinterdorfer, P., Baber, G., and Tamm, L. K. (1995) *EMBO J. 14*, 5514−5523.
40. Gray, C., and Tamm, L. K. (1997) *Protein Sci. 6*, 1993−2006.
41. Gray, C., and Tamm, L. K. (1998) *Protein Sci. 7*, 2359−2373.

BI991232H